Research Article

Journal of Environmental Nanotechnology

# Impact of Tin and Titanium Doping on Acetone Gas Sensing Properties of Vanadium Dioxide Thin Films

Karthikadevi Krishnasamy[1], Samidurai Thangavel[1], Prabahar Subramaniam[1], Srikanth Srinivasan[2], Sridharan Madanagurusamy[3,4] and Karunanithi Udayar[1,5*]

[1]PG & Research Department of Physics, Government Arts College, Udumalpet, Tiruppur, TN, India
[2]Department of Physics, Chikkanna Government Arts College, Tirupur, TN, India
[3]Functional Nanomaterials & Devices Lab, School of Electrical & Electronics Engineering, SASTRA Deemed University, Thanjavur, TN, India
[4]School of Arts, Science, Humanities and Education, SASTRA Deemed University, Thanjavur, TN, India
[5]Department of Physics, Sri Meenakshi Government Arts College for Women, Madurai, TN, India
Received: 29.03.2025 Accepted: 08.05.2025 Published: 30.06.2025
*karunanithiu30@gmail.com

## ABSTRACT

Room-temperature operable gas sensors with remarkable sensitivity, selectivity, and dependability have become a necessity to handle the rising hazards associated with the emissions of dangerous volatile organic compounds. Metal oxide thin films are desirable as chemi-resistive gas sensors because of their selectivity, large reactive surface area, and tunability of physicochemical characteristics. Vanadium dioxide ($VO_2$) has remarkable promise as a gas sensing material due to its catalytic and physicochemical properties. This work develops an efficient technique for manufacturing extremely porous and oxygen vacancy-enriched Ti and Sn-doped $VO_2$ thin films to address issues of partial physisorption and protracted reactions. Tin-doping reduced the optical bandgap from 3.60 eV (undoped) to 3.18 eV. The Sn-doped $VO_2$ film showed improved acetone gas sensing abilities, achieving a sensitivity of 330% and response/recovery times of 20/60 seconds at 500 ppm. The improved performance is due to the augmented reactive surface area and elevated density of defect-induced oxygen vacancies facilitated by Sn doping. These results suggest that Sn-doped $VO_2$ thin films may serve as valuable materials for the development of industrial safety devices.

**Keywords**: $VO_2$ films; Chemical bath deposition; Sensors; Acetone; Physisorption.

## 1. INTRODUCTION

Gas sensors are extensively utilized and essential across the fields of environmental monitoring, healthcare and food quality assessment applications. Due to industrial expansion and pollution, environmental monitoring has gained prominence (Das *et al*. 2022; Maheswari *et al*. 2020; Nikolic *et al*. 2020). For monitoring hazardous gases in the environment, many researchers have tried to fabricate small, easy-to-use, reasonably priced, and extremely stable sensors (Maheswari *et al.* 2020). Consequently, a variety of gas sensors are designed and constructed to satisfy detection needs and to optimize their functioning. These gas sensors include optical, acoustic, electrochemical, and semiconductor gas sensors (Panda *et al.* 2024). Due to their low complexity, rapid response, stability, sensitivity, and simplicity of production, chemi-resistive nano metal oxide gas sensors exhibit excellent potential for a wide range of real-world applications (Dey, 2018). Metal oxide thin film-based gas sensors have directly or indirectly contributed to newer research areas in the field of solid-state. These developments are largely due to their unique structural (Table 1), geometrical and thickness-dependent properties (Xavier and Sivaperuman, 2024). Nanostructured metal oxide thin films are highly sensitive to low detection limits because of their massive surface modification, enormous surface area-to-volume ratio and their particle size comparable to that of gas molecules. While thin film sensors are useful, their performance at high temperatures limits their service life, reduces stability, and increases energy consumption. Thus, research into gas-sensitive materials operating at ambient temperature has drawn interest to find a solution to this critical challenge (Alagarasan *et al.* 2025). One of the significant n-type oxide semiconductors is vanadium dioxide ($VO_2$) that can undergo phase transformations depending on the environment. The metastable monoclinic phase structure of $VO_2$ (M) has attracted a lot of interest recently because of its sensitive room-temperature performance toward gases and its consistent large band gap. The enormous surface area-to-volume ratio of $VO_2$ and its composite oxides make them suitable for future applications in sensor technology (Liang *et al.* 2022b). Reports in the literature have detailed the nanostructures of $VO_2$, including nanowires (Liang *et al.* 2022a), nano grooves (Hien *et al.* 2021) and nanorods (Liang *et al.* 2022b), for the detection of $NO_2$, ammonia, and $H_2S$. These $VO_2$ sensors are fabricated through intricate synthesis and deposition processes. Thus, there

is a significant demand for the development of effective, simple and inexpensive sensing materials through a facile fabrication method. Through the use of doping and forming heterojunctions with metals and metal oxides, it has been possible to overcome these issues. Ag-modified $VO_2$ nanorods were produced through the use of a hydrothermal process in order to detect $NO_2$. In addition to the modification of the energy band gap and triggered catalytic effect of silver nanoparticles enhance the sensing capability of the $VO_2$ nanorods (Liang *et al.* 2022c). To improve the performance of the room temperature sensor, a straightforward hydrothermal process was used to fabricate $VO_2$ nanorods composited with rGO in a flake form (Liang *et al.* 2022b). In the present work, an effort was made to synthesize $VO_2$ thin films and enhance their acetone gas sensing capabilities by Sn and Ti doping.

## 2. EXPERIMENTAL SECTION

Tin chloride, titanium isopropoxide, ammonia meta vanadate, hydrogen peroxide, acetone, glass substrates, and distilled water were acquired from Sigma Aldrich Co. Ltd. Powdered vanadium pentoxide was made from thermal decomposition method by annealing ammonia metavanadate at 450°C for two hours in a muffle furnace (Shafeeq *et al.* 2020). Using the ultrafast chemical deposition process, doped and pure $VO_2$ thin films were fabricated. Vanadium pentoxide (0.56 g) powder was dissolved in 30 mL of hydrogen peroxide, followed by vigorous stirring for 20 minutes to produce a homogeneous orange solution. The resultant solution was heated to 70°C and maintained for 30 seconds. Following completion of the reaction, the cleaned glass substrates were soaked in the solution for 30 minutes. Subsequently, the deposited $VO_2$ thin films were air-dried for one day and annealed at 100°C for a period of 4 hours. The Sn and Ti-doped $VO_2$ thin films were produced using the same technique, with the incorporation of Sn and Ti by adding appropriate amount of tin chloride and titanium isopropoxide. The impact of Sn and Ti on $VO_2$ thin films were studied using XRD, UV-VIS, SEM, PL and gas sensing analysis.

A homemade gas sensing system was used for the gas sensing investigations. For the purpose of conducting sensing test, $VO_2$ thin films with dimensions of 1 cm × 1 cm were utilized. The $VO_2$ sensing electrode was fabricated by pasting the copper wire on the sensing film surface by the use of silver paste. Finally, the designed sensing electrodes were subjected to heat treatment utilizing the sodium vapor lamp. The prepared $VO_2$ sensing electrodes were placed in a 1-L sensing chamber and filled with both target gases and ordinary air. The film was linked to a Keithley 6517B electrometer through ohmic contacts. The current variations in the presence and absence of target gases were meticulously recorded and analyzed using a 5-V bias voltage. After injecting target gas at varying concentrations (50, 100, 250 and 500 ppm), the resistance of the film was continually measured as a function of time. This was done in order to get the desired results. The same process was carried out for each of the pure and doped $VO_2$ films. The relative response was calculated using equation (1).

$$\text{Response (S\%)} = \left(\frac{R_a}{R_g} \text{ x100 }\right) \quad \text{... (1)}$$

## 3. RESULTS AND DISCUSSION

### 3.1 X-ray Diffraction Studies

X-ray diffraction was used to study the crystallinity and phase of both pure and doped samples of $VO_2$ thin films. As can be observed in Fig. 1, a sequence of peaks emerges at 2θ values of 27.87°, 36.48°, 41.77°, 54.70° and 57.14° respectively. These peaks correspond to the characteristic diffraction peaks of (011), (200), (210), (102) and (300) lattice planes of $VO_2$ with a monoclinic structure. These peaks are in good agreement with the standard PDF card of $VO_2$ (JCPDS No.44-0252). The purity of every sample was confirmed by the absence of any additional impurity diffraction peaks. Sn and Ti-doped films show a noticeable left shift in the diffraction peaks that correspond to the (011) plane. In accordance with the inference of Bragg's rule, this occurrence may be accounted for by the differential radius of the V ion and doped (Sn and Ti) ions. Compared to Sn and Ti ions, the ionic radius of V ions is 0.59 Å, which is smaller. Since the lattice grows in response to the addition of the doped ion, the (011) diffraction peak moves to a smaller angle. Also, the incorporation of Sn and Ti decreases the strength of the diffraction peaks. This is likely due to an increase in crystal defects (Sinha 2019).

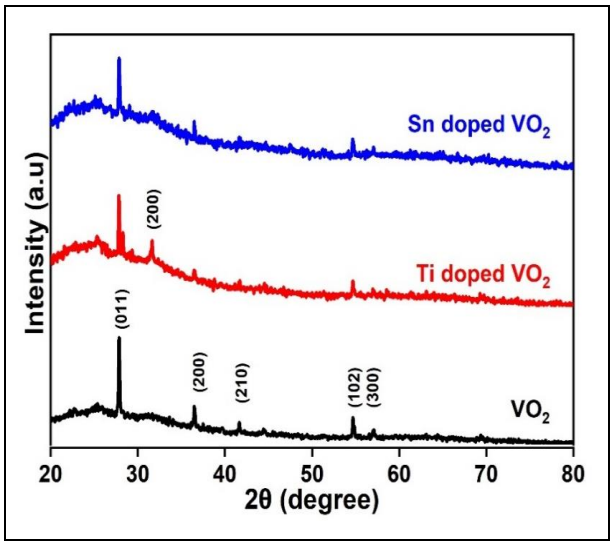



**Fig. 1: XRD pattern for pure and doped $VO_2$ thin films**

**Table 1. Structural parameters of pure and doped $VO_2$ thin films**

| Sample | Lattice Constant (Å) | Grain Size (D) (nm) | Dislocation Density (δ) ($\times 10^{10}$ lines/m$^2$) | Micro Strain (ε) ($\times 10^{-3}$) | Band Gap ($E_g$) (eV) | Response (S%) |
|---|---|---|---|---|---|---|
| $VO_2$ | 4.5350 | 170 | 0.000004 | 0.000226 | 4.04 | 156 |
| Ti-doped $VO_2$ | 4.5344 | 127 | 0.000008 | 0.000301 | 3.83 | 233 |
| Sn-doped $VO_2$ | 4.5336 | 102 | 0.000012 | 0.000376 | 3.59 | 350 |

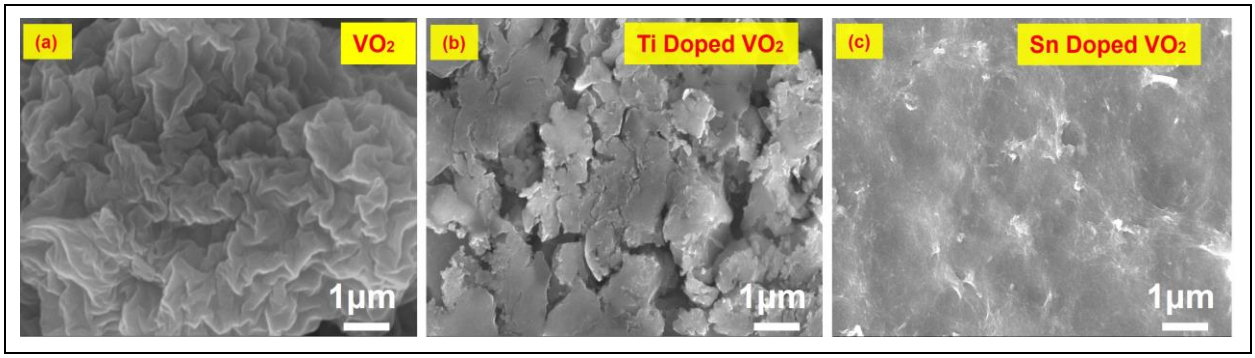



**Fig. 2: SEM images of (a) $VO_2$, (b) Ti-doped $VO_2$ and (c) Sn-doped $VO_2$ thin films**

## 3.2 Morphological Study

The film morphology has a significant impact on the performance of the gas sensor in metal oxide semiconductors. The SEM pictures Fig. 2 (a–c) clearly show the difference between the surface features of pure $VO_2$, Ti-doped $VO_2$ and Sn-doped $VO_2$ films. When Ti is added, the porous structure starts to get bigger and holes appear in the thin film sample. Similar porous surface shape was observed on the Sn-doped $VO_2$ film. Particles were not tightly packed in Sn-doped films when compared to Ti-doped films, which may help the target gas diffusion (Thangavel *et al.* 2024).

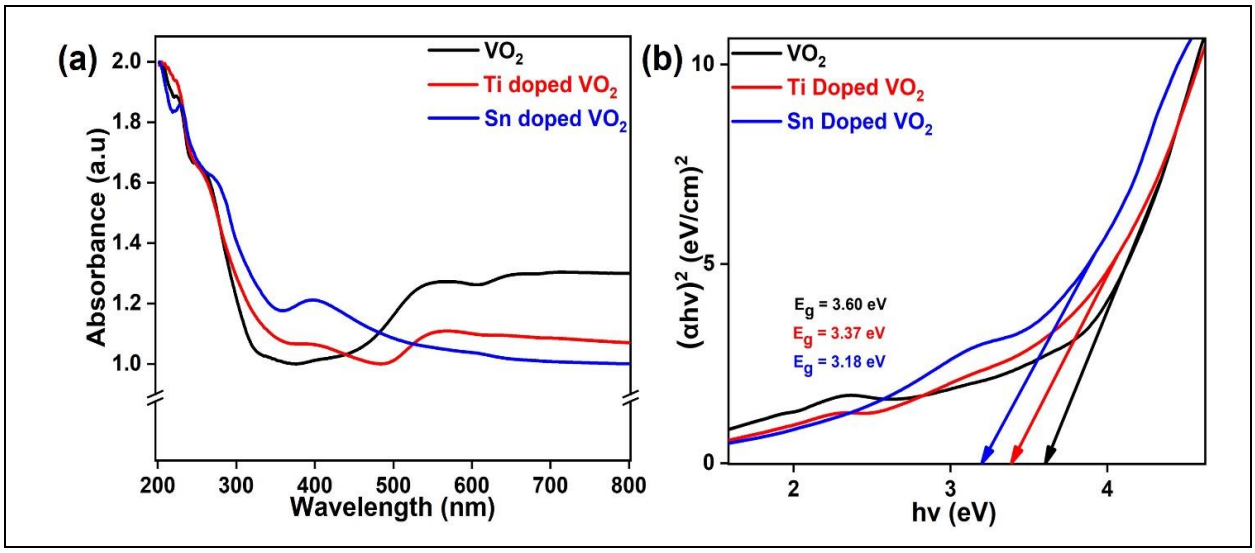



**Fig. 3: UV-DRS spectroscopy of (a) absorption, (b) Tauc's plot of pure and doped $VO_2$ thin films**

## 3.3 Optical Characterization

The optical characteristics of pure Ti-doped and Sn-doped $VO_2$ thin films were evaluated using a UV-Vis-NIR spectrophotometer. Fig. 3a displays the absorption spectra of $VO_2$ films within the wavelength range 200-800 nm. The absorption of $VO_2$ films is enhanced by doping. The increased absorption seen for doped films

may be ascribed to the enhanced scattering of photons due to crystal defects and surface roughness induced by doping. The bandgap energies for pure, Ti-doped, and Sn-doped $VO_2$ thin films were evaluated *via* Tauc's plot illustrated in Fig. 3b. The band gap value for pure $VO_2$ film was 3.60 eV, whereas it was reduced to 3.37 eV and 3.18 eV for the Ti and Sn-doped films, respectively. The findings indicate that the reduction in bandgap energies is attributed to the incorporation of Ti and Sn metals within the $VO_2$ thin film lattice.

## 3.4 Photoluminescence Properties

The defect levels, recombination process, and quality of the manufactured thin films were investigated by photoluminescence (PL) measurement. This was carried out using an excitation source with the wavelength of 325 nm. The PL spectra of pure and doped $VO_2$ thin films are shown in Fig. 4. These spectra were acquired at room temperature in the wavelength range 290-470 nm. Five emission peaks around 305 nm, 380 nm, 395 nm, 457 nm and 467 nm can be observed in Fig. 4. The incorporation of Sn and Ti in $VO_2$ lattice impacts the PL intensity, owing to the less crystallinity and the formation of surface detects. The PL spectrum shows an emission peak at 305 nm (4.06 eV), which is very close to the calculated bandgap of pure thin film. This is due to free-exciton recombination, which leads to near-band edge emission. The emission bands at 380, 395, 457 and 467 nm may be attributed to radiative transitions mediated by distinct defect states within the bandgap, primarily generated by oxygen vacancies. The luminous peak at 305 nm is much less intense in both pure and Ti-doped $VO_2$ thin films. Decreased crystallinity with oxygen vacancies of Sn-doped $VO_2$ thin films is beneficial for gas sensor application. The results are in good agreement with XRD data.

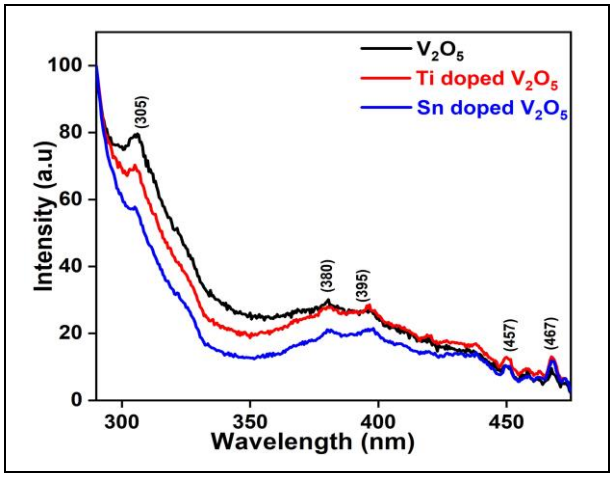



**Fig. 4: PL spectra for pure and doped $VO_2$ thin films**

**Table 2. Comparison of the present work with available reports**

| S. No. | Thin Films | Operating Temperature (°C) | Response (S) | Response Time (Sec) / Recovery Time (sec) | Source |
|---|---|---|---|---|---|
| 1 | $WO_3$ | 300 | 16 | 45 / 251 | (Drmosh *et al.* 2021) |
| 2 | $VO_2$ | RT | 97 | 49 / 19 | (Ezhilan *et al.* 2021) |
| 3 | $VO_2$ | RT | 93 | 10 / 21 | (Qin *et al.* 2024) |
| 4 | $Ti^{3+}$-doped CdO | 130 | 10 | - | (Velusamy *et al.* 2022) |
| 5 | $VO_2$ | RT | 4 | - | (Vijayakumar *et al.* 2021) |
| 6 | Sn-doped $VO_2$ | RT | 350 % | 20 / 65 | Present work |

RT: Room temperature; Response (S) $= \frac{R_a}{R_g}$ , Response (S%) $= \frac{R_a}{R_g} \times 100$

## 3.5 Acetone Gas Sensing Performance of $VO_2$ Thin Films

The bar diagram (Fig. 5a) displays the response of pure and doped $VO_2$ thin films on exposure to 500 ppm concentration of acetaldehyde, ethanol, xylene, butanol and acetone at room temperature. It was observed that $VO_2$ sensing films responded highly to acetone than other target gases. The response of $VO_2$ sensing films was poor with the values being below 50% for acetaldehyde, ethanol, xylene and butanol. The obtained response values indicate that the prepared films are more sensitive and selective to acetone due to the monoclinic crystal structure (Thangavel *et al.* 2024). Fig. 5(b-d) show the resistance graphs of the prepared $VO_2$ thin films. Among all the films Sn-doped film exhibits high response to acetone at 500 ppm.

In order to know more about the acetone detecting property, Sn-doped $VO_2$ film was extensively utilized in further gas sensing tests. Utilizing acetone vapors at concentrations of 50, 100, 250 and 500 ppm, the transient response-recovery behavior of the Sn-doped $VO_2$ sensors was examined Fig. 6 (a). As the acetone concentration rose (50-500 ppm), Sn-doped $VO_2$ sensor reaction was also found to rise, suggesting that the amount of acetone molecules in the exposure was gradually escalating (Mounasamy *et al.* 2018). The results show that the Sn-doped $VO_2$ sensors are highly reducing and have an n-type response to acetone. On the other hand, as acetone exposure increased, the sensing

element's reaction speed got accelerated. Fig. 6a shows the response (20 s) and recovery (65 s) signals of the Sn-doped $VO_2$ sensors. These sensors exhibited short-term response time towards 500 ppm acetone gas. These results suggest that the Sn-doped $VO_2$ sensors can be successfully used in acetone gas sensors (Drmosh *et al*. 2021; Ezhilan *et al*. 2021;Qin *et al*. 2024).

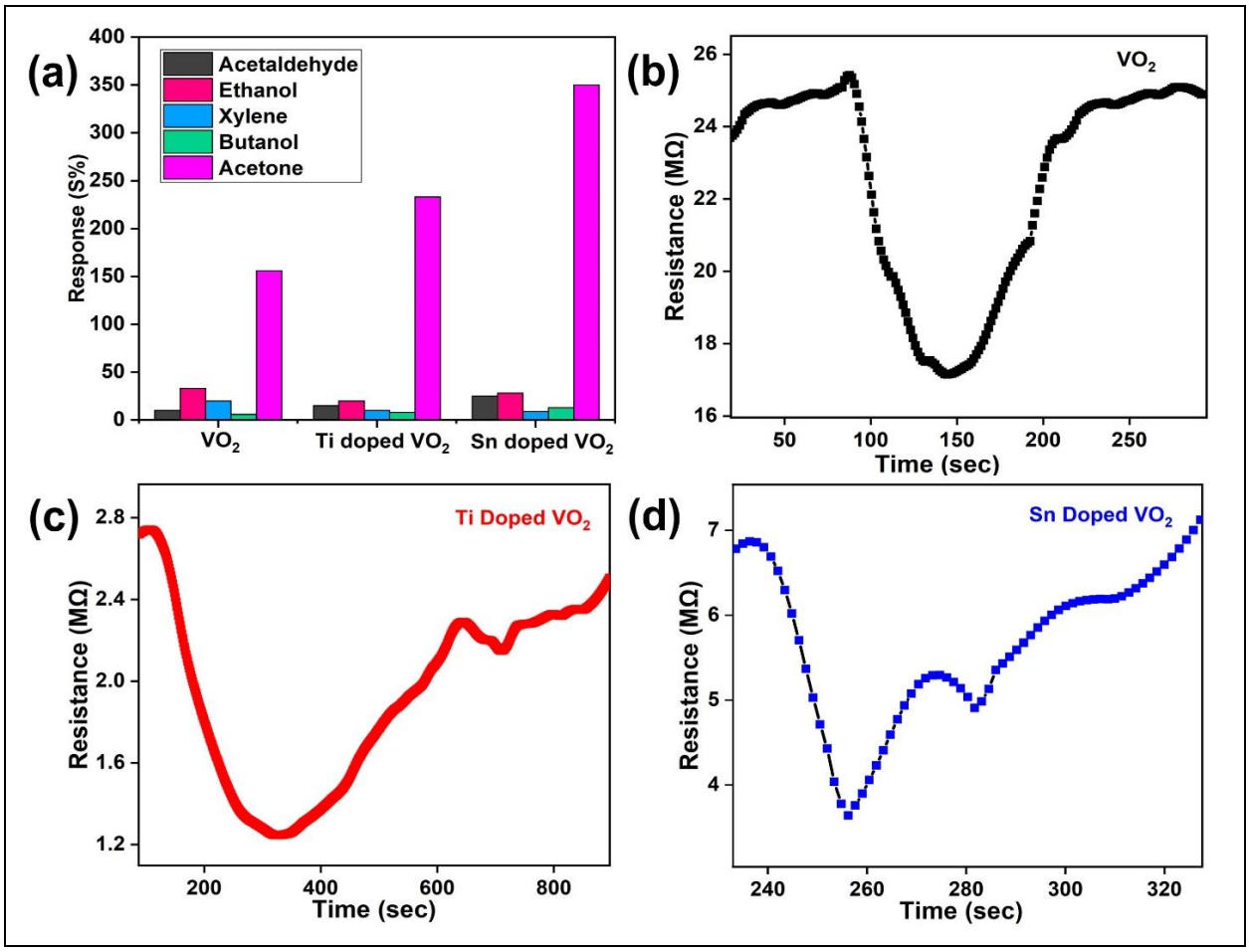



**Fig. 5: (a) Response comparison of pure and doped $VO_2$ thin films, Response curves of (b) $VO_2$, (c) Ti-doped $VO_2$ and (d) Sn-doped $VO_2$ thin films**

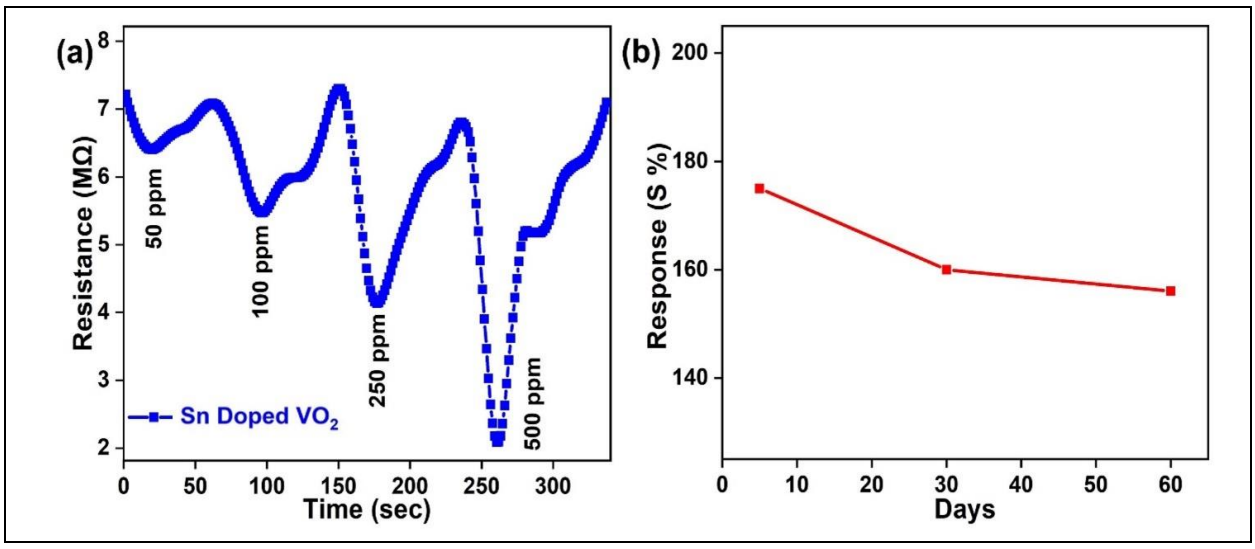



**Fig. 6: (a) Transient response and (b) stability curves of Sn-doped $VO_2$ thin films**

Since the Sn-doped $VO_2$ sensors showed enhanced sensitivity, they were evaluated for structural, morphological, and optical properties. Surface defects of Sn-doped $VO_2$ sensors were conformed from the XRD and SEM results which encouraged the penetration of acetone. The smallest grain size (102 nm), highest dislocation density and lattice strain of Sn-doped $VO_2$ sensors creates the additional absorption sites for acetone, enhancing the response. The imperfections in the lattice have the potential to function as centers of entrapment and increase the sensitivity. This was also confirmed by the PL and UV absorbance spectra. The formation of the intermediate band was the result of imperfections. This contributes towards the creation of adsorption sites that are used by the target molecules (Alagarasan *et al.* 2025). Moreover, there was a notable decrease in resistivity and a drop in the carrier concentration when the Sn-doping was introduced. Moreover, larger proportion of oxygen vacancy in Sn-doped $VO_2$ sensors resulted in the generation of extra active sites on its surface (Thangavel *et al.* 2024). This enhanced interactions between gas molecules and the sensing material, which led to an improvement in sensing capabilities. Through the modulation of charge dynamics in both the adsorption and desorption mechanisms, it is concluded that the introduction of Sn in the $VO_2$ lattice has a significant role in improving the performance of gas sensing kinetics. Owing to this reason, the response of Sn-doped $VO_2$ sensors to acetone might be high. Table 2 presents a comparison of the sensor responses of various acetone sensors documented in the literature with the results of the current study.

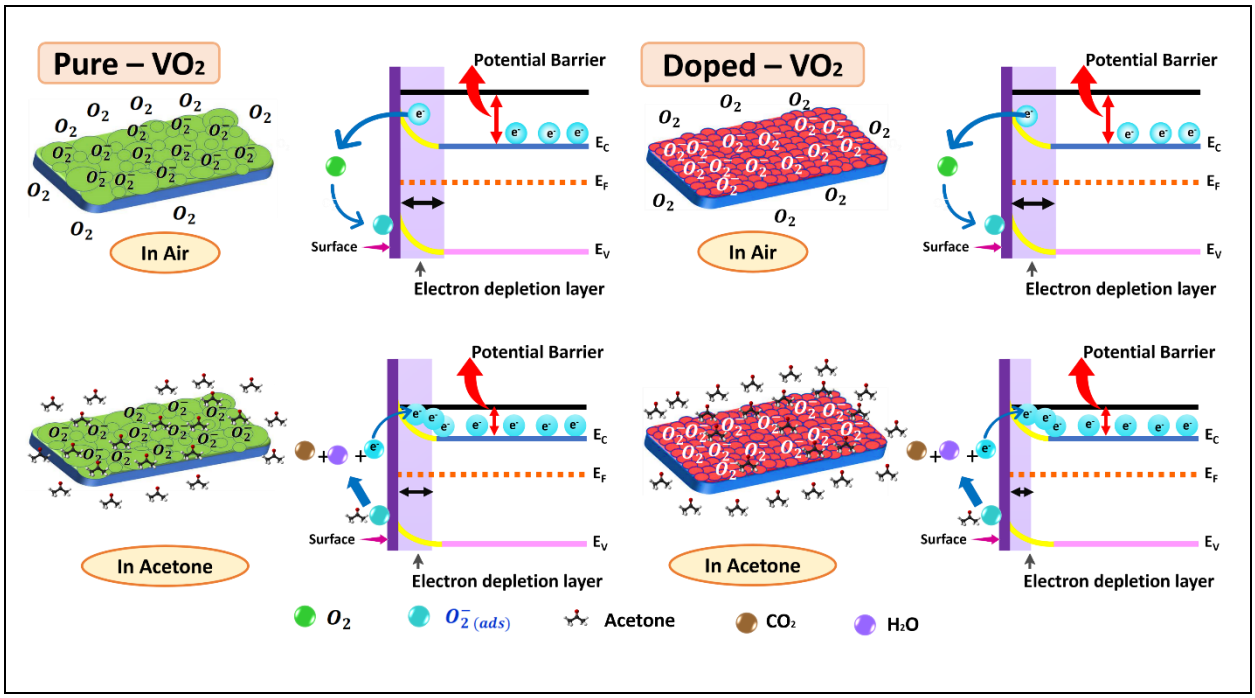



**Fig. 7: Schematic diagram of sensing mechanism of pure and doped $VO_2$ thin film sensor**

## 3.6 Sensing Mechanism

Interaction between acetone molecules and Sn-doped $VO_2$ thin film is depicted in Fig. 7. In the air, Sn doped $VO_2$ sensors absorb oxygen molecules from the atmosphere and get free electrons of Sn-doped $VO_2$ sensors to create oxygen ion species ($O_{2(ads)}$, and $O^-_{2(ads)}$). Hence, the surface developed an electron depletion layer, increasing the resistance of the Sn-doped $VO_2$ sensors ($R_a$). Adsorbed oxygen ions react with acetone species after they get into contact with them, producing $CO_2$ and $H_2O$ ($R_g$). This lowers the potential barrier to the formation of a narrow electron depletion area by returning trapped electrons back into the Sn-doped $VO_2$ sensor. As a result, the sensor's resistance drop. The following is the reaction sequence:

$$O_2 \longrightarrow O_{2(ads)} \quad \ldots (1)$$

$$O_{2(ads)} + e^- \longrightarrow O^-_{2(ads)} \quad \ldots (2)$$

$$(CH_3)_2CO + 4\,O_{2(ads)} + 3O^-_{2(ads)} \longrightarrow 3CO_2\uparrow + 3H_2O\uparrow + 4e^- \quad \ldots (3)$$

## 4. CONCLUSION

Chemical bath deposition process was utilized to prepare pure Sn and Ti-doped $VO_2$ thin films, which were then investigated for their potential in acetone gas sensing applications. The introduction of doping significantly modified the microstructure and surface morphology of the $VO_2$ thin films. The XRD analysis revealed a significant reduction in the crystallinity of $VO_2$ films due to Ti and Sn doping. SEM micrographs revealed a nanograin porous microstructure in the Sn-doped $VO_2$ thin film. Sn-doping on $VO_2$ demonstrated a

reduction in the optical bandgap from 3.60 eV for the undoped $VO_2$ thin film to 3.18 eV. The PL spectra indicated the existence of oxygen vacancy defects in the Sn-doped $VO_2$ film, which enhances the gas sensing performance. Sn-doped $VO_2$ film displayed optimal performance as a sensing material for acetone gas at room temperature. The favorable sensing response of 330% and the response/recovery time of 20/60s at a 500 ppm acetone concentration suggests that Sn-doped $VO_2$ thin films may serve as a valuable material for the development of industrial safety devices.

## FUNDING

There is no funding source.

## CONFLICT OF INTEREST

The authors declared no conflict of interest in this manuscript regarding publication.

## COPYRIGHT

This article is an open-access article distributed under the terms and conditions of the Creative Commons Attribution (CC BY) license (http://creativecommons.org/licenses/by/4.0/).



## REFERENCE

Alagarasan, D., Hegde, S. S., Naik, R., Shetty, H. D., Prasad, H. B. S., Alshahrani, T., AlFaify, S. and Shkir, Mohd., Remarkable NH3 gas sensing performance of spray deposited Tb doped WO3 thin films at room temperature, *J. Photochem. Photobiol. A Chem.*, 459, 116087(2025). https://doi.org/10.1016/j.jphotochem.2024.116087

Das, S., Mojumder, S., Saha, D. and Pal, M., Influence of major parameters on the sensing mechanism of semiconductor metal oxide based chemiresistive gas sensors: A review focused on personalized healthcare, *Sens. Actuators B Chem.*, 352, 131066(2022). https://doi.org/10.1016/j.snb.2021.131066

Dey, A., Semiconductor metal oxide gas sensors: A review, *Mater. Sci. Eng. B-Adv.* 229, 206–217(2018). https://doi.org/10.1016/j.mseb.2017.12.036

Drmosh, Q. A., Al-Muhaish, N. A., Wajih, Y. A. Al., Alam, M. W., and Yamani, Z. H., Surface composite and morphology tuning of tungsten oxide thin films for acetone gas sensing, *Chem. Phys. Lett.*, 776, 138659(2021). https://doi.org/10.1016/j.cplett.2021.138659

Ezhilan, M., J. B. B, A. J. and Rayappan, J. B. B., Influence of PVA templates on the synthesis of interconnected and long-winded electrospun $V_2O5$ nanowires – Acetone sensor, *Mater. Res. Bull.*, 139, 111276(2021). https://doi.org/10.1016/j.materresbull.2021.111276

Hien, V. X., Thang, T. M., Dong, V. T., Nhat, D. D., Nghi, N. T., Phuoc, L. H., Khoa, C. T., Vuong, D. D. and Chien, N. D., Synthesis of $VO_2$ thin films from vanadium powder and determination of room-temperature $NH_3$ sensing properties, *J. Mater. Sci.: Mater. Electron.*, 32(10), 13803–13812(2021). https://doi.org/10.1007/s10854-021-05956-w

Liang, J., Wang, K., Xuan, C., Chen, Q., Tai, W., Ge, P. and Zhang, H., Room temperature $H_2S$ gas sensing performance of $VO_2$(A) nanowires with high aspect ratio, *Sens. Actuators A Phys.*, 347, 113986(2022a). https://doi.org/10.1016/j.sna.2022.113986

Liang, J., Wu, W., Lou, Q., Wang, K. and Xuan, C., Room temperature $NO_2$ sensing performance enhancement of $VO_2$(B) composited rGO structure, *J. Mater. Sci.: Mater. Electron.*, 33(19), 15473–15482(2022b). https://doi.org/10.1007/s10854-022-08454-9

Liang, J., Wu, W., Lou, Q., Wang, K. and Xuan, C., Room temperature $NO_2$ sensing performance of Ag nanoparticles modified $VO_2$ nanorods, *J. Alloys Compd.*, 890, 161837(2022c). https://doi.org/10.1016/j.jallcom.2021.161837

Maheswari, S., Karunakaran, M., Kasirajan, K., Chandrasekar, L. B. and Boomi, P., Yttrium - Substituted $SnO_2$ thin films and its gas sensing activity against $NH_3$ gas: Characterization and sensitivity evaluation, *Sens. Actuators A Phys.*, 315112303(2020). https://doi.org/10.1016/j.sna.2020.112303

Mounasamy, V., Mani, G. K., Ponnusamy, D., Tsuchiya, K., Prasad, A. K. and Madanagurusamy, S., Template-free synthesis of vanadium sesquioxide ($V_2O_3$ ) nanosheets and their room-temperature sensing performance, *J. Mater. Chem. A Mater.*, 6(15), 6402–6413(2018). https://doi.org/10.1039/C7TA10159G

Nikolic, M. V., Milovanovic, V., Vasiljevic, Z. Z. and Stamenkovic, Z., Semiconductor Gas Sensors: Materials, Technology, Design, and Application, *Sensors*, 20(22) 6694(2020). https://doi.org/10.3390/s20226694

Panda, S., Mehlawat, S., Dhariwal, N., Kumar, A. and Sanger, A., Comprehensive review on gas sensors: Unveiling recent developments and addressing challenges, *Mater. Sci. Eng. B-Adv.* 308, 117616(2024). https://doi.org/10.1016/j.mseb.2024.117616

Qin, Y., Wang, H., Zhou, C., and Bai, Y., Microflowers Composed of $VO_2$ Nanoflakes for Selective Detection of Acetone and Ammonia, *ACS Appl. Nano. Mater.*, 7(6), 5853–5861(2024). https://doi.org/10.1021/acsanm.3c05179

Shafeeq, K. M., Athira, V. P., Kishor, C. H. R. and Aneesh, P. M., Structural and optical properties of $V_2O_5$ nanostructures grown by thermal decomposition technique, *Appl. Phys. A-Mater.*, 126(8), 1-6(2020). https://doi.org/10.1007/s00339-020-03770-5

Sinha, S. K., Effect of temperature on structural, optical and electrical properties of pulsed-laser deposited W-doped $V_2O_5$ thin films, *Superlattices Microstruct.*, 12588–94(2019). https://doi.org/10.1016/j.spmi.2018.10.029

Thangavel, S., Pattappan, D., Subramaniam, P., Srinivasan, S., Madanagurusamy, S., Krishnasamy, K., Lai, Y. -T. and Udayar, K., Defect-enabled room-temperature acetone gas sensors based on Zn-doped cauliflower-like bismuth oxide, *Ceram. Int.*, 50(19), 36512–36520(2024). https://doi.org/10.1016/j.ceramint.2024.07.037

Velusamy, P., Babu, R. R., Sathiya, M., Ahmad, A., Alothman, A. A., Mushab, M. S. S., Elamurugu, E., Pandian, M. S. and Ramasamy, P., Incorporation of $Ti^{3+}$ metal ions in chemically spray deposited CdO thin films for optoelectronic and chem-resistive based formaldehyde gas sensor applications, *New J. Chem.* 46(46), 22469–22485(2022). https://doi.org/10.1039/D2NJ02925A

Vijayakumar, Y., Nagaraju, P., Sreekanth, T., Rushidhar, U. and Reddy, P. S., Effect of precursor volume on chemically sprayed $V_2O_5$ thin films for acetaldehyde detection, *Superlattices Microstruct.*, 153, 106870(2021). https://doi.org/10.1016/j.spmi.2021.106870

Xavier, R. and Sivaperuman, K., Review on the of physical vapor deposition on imminent chemiresistive metal oxide gas sensors and their future scope, *Mater. Today Commun.*, 38, 107831(2024). https://doi.org/10.1016/j.mtcomm.2023.107831